JOURNAL OF VIROLOGY, Jan. 2003, p. 841–850 Vol. 77, No. 2
0022-538X/03/$08.00+0 DOI: 10.1128/JVI.77.2.841–850.2003


# The N-Terminal Domain of the Murine Coronavirus Spike Glycoprotein Determines the CEACAM1 Receptor Specificity of the Virus Strain

Jean C. Tsai,[1] Bruce D. Zelus,[2] Kathryn V. Holmes,[2] and Susan R. Weiss[1]*

*Department of Microbiology, University of Pennsylvania School of Medicine, Philadelphia, Pennsylvania 19104,[1] and Department of Microbiology, University of Colorado Health Sciences Center, Denver, Colorado 80626[2]*

Received 25 June 2002/Accepted 15 October 2002

**Using isogenic recombinant murine coronaviruses expressing wild-type murine hepatitis virus strain 4 (MHV-4) or MHV-A59 spike glycoproteins or chimeric MHV-4/MHV-A59 spike glycoproteins, we have demonstrated the biological functionality of the N-terminus of the spike, encompassing the receptor binding domain (RBD). We have used two assays, one an in vitro liposome binding assay and the other a tissue culture replication assay. The liposome binding assay shows that interaction of the receptor with spikes on virions at 37°C causes a conformational change that makes the virions hydrophobic so that they bind to liposomes (B. D. Zelus, J. H. Schickli, D. M. Blau, S. R. Weiss, and K. V. Holmes, J. Virol. 77: 830–840, 2003). Recombinant viruses with spikes containing the RBD of either MHV-A59 or MHV-4 readily associated with liposomes at 37°C in the presence of soluble mCEACAM1$^a$, except for $S_4$R, which expresses the entire wild-type MHV-4 spike and associated only inefficiently with liposomes following incubation with soluble mCEACAM1$^a$. In contrast, soluble mCEACAM1$^b$ allowed viruses with the MHV-A59 RBD to associate with liposomes more efficiently than did viruses with the MHV-4 RBD. In the second assay, which requires virus entry and replication, all recombinant viruses replicated efficiently in BHK cells expressing mCEACAM1$^a$. In BHK cells expressing mCEACAM1$^b$, only viruses expressing chimeric spikes with the MHV-A59 RBD could replicate, while replication of viruses expressing chimeric spikes with the MHV-4 RBD was undetectable. Despite having the MHV-4 RBD, $S_4$R replicated in BHK cells expressing mCEACAM1$^b$; this is most probably due to spread via CEACAM1 receptor-independent cell-to-cell fusion, an activity displayed only by $S_4$R among the recombinant viruses studied here. These data suggest that the RBD domain and the rest of the spike must coevolve to optimize function in viral entry and spread.**

Mouse hepatitis virus (MHV) is a murine coronavirus capable of infecting the liver, the central nervous system, and other internal organs, depending on the virus strain and the mouse strain. The observations that coronavirus infection is highly host species specific and MHV pathogenesis is virus strain specific have led to investigations of the viral and host determinants of pathogenesis. We have used two neurotropic strains in this study. MHV-4 is a highly neurovirulent isolate of the JHM strain that does not cause significant hepatitis; MHV-A59 is a less neurovirulent strain which causes moderate to severe hepatitis (29, 30, 50).

Murine carcinoembryonic antigen-related cell adhesion molecules (mCEACAMs; CD66a, previously known as mmCGM or Bgp), serve as receptors that mediate MHV entry (3, 14, 36, 54). Members of the CEA family are involved in intercellular adhesion and the development of hepatocellular, colorectal, and epithelial tumors (3). mCEACAMs are glycoproteins of two or four immunoglobulin-like extracellular domains followed by a transmembrane domain and a long or short cytoplasmic tail. MHV binding activity has been mapped to the N-terminal domain of CEACAM1$^a$ (16, 41, 52).

The MHV receptor glycoproteins are encoded by two murine *ceacam* genes, m*ceacam*1 and m*ceacam*2 (14, 36). Murine *ceacam*1 is expressed as allelic glycoproteins, mCEACAM1$^a$ and mCEACAM1$^b$, which differ in 27 of the 108 amino acids in the N-terminal immunoglobulin-like domain(14). The proteins are expressed as four-domain and two-domain isoforms primarily on the epithelial and endothelial cells of the respiratory tract and the intestines and other tissues (21, 42, 45). Murine CEACAM2 isoforms contain two immunoglobulin-like domains and have 48% amino acid sequence identity to the N-terminal domain of mCEACAM1$^a$ (36). The four-domain mCEACAM1$^a$ isoform (called mCEACAM1$^a$[1–4]) and the two-domain mCEACAM1$^a$ (called mCEACAM1$^a$[1,4]) are more efficient receptors for MHV-A59 than are mCEACAM1$^b$[1–4], mCEACAM1$^b$[1,4] and mCEACAM2 (14, 35, 36, 41, 56). Although the biological requirements for an efficient MHV receptor are not known, these data are consistent with reports of the relative resistance to MHV infection of the SJL/J mouse, which contains only the mCEACAM1$^b$ allele (14, 37, 54).

The MHV surface glycoprotein spike (S) mediates many biological properties of MHV, including receptor attachment, fusion of viral and cell membranes during entry, cell-to-cell fusion during viral spread, and immune activation (5). Spike is a type I membrane protein of approximately 180 kDa. On the MHV-A59 and MHV-4 virions, S is cleaved posttranslationally into two approximately 90-kDa subunits, the amino-terminal S1 and the carboxy-terminal S2 (5): S1 binding to mCEACAM is thought to induce structural rearrangements within spike

* Corresponding author. Mailing address: Department of Microbiology, 203A Johnson Pavilion, 36th and Hamilton Walk, University of Pennsylvania, Philadelphia, PA 19104-6076. Phone: (215) 898-8013. Fax: (215) 573-4858. E-mail: weisssr@mail.med.upenn.edu.

that are necessary for subsequent fusion of cell and viral membranes (26, 51, 55). S2 contains two or three heptad repeat domains, as well as a putative fusion peptide, believed to mediate fusion (11, 19, 26, 32, 33, 47). Among the MHV strains, S2 is relatively conserved and S1 is more variable (46). MHV-A59 and MHV-4 have 96% amino acid identity in S2 and 85% amino acid identity in S1.

Abundant evidence points to virus entry as the primary barrier to host range restriction of coronavirus replication (4, 7, 12, 49, 53). Nonpermissive cell lines of many nonmurine species, such as hamster, pig, and human, become readily susceptible to productive MHV infection once they are transfected to express mCEACAM1 glycoproteins (14, 16). Viruses from persistently- infected murine 17Cl-1 cells, murine DBT cells, or mixed DBT-BHK cell cultures displayed extended host range in cell culture; such viruses had mutations in the spike protein that altered viral interactions with mCEACAM1, and some of these (as well as some MHV strains) were able to use human CEACAM(1, 2, 6). Furthermore, chimeric coronaviruses, generated by targeted RNA recombination, expressing spike glycoproteins from other coronavirus strains demonstrate the pathogenic properties or host tropism of the strain from which the spike was derived (10, 28, 40, 44).

The N terminus of the spike protein has been implicated in virus-receptor interactions. The N-terminal 330 amino acids of S1, expressed as a truncated protein, has the ability to bind to mCEACAM1$^a$ blotted onto membranes and has been referred to as the receptor binding domain (RBD) (27, 48). Amino acid substitutions within the RBD can have major effects on receptor utilization and infection. For example, L65H, was identified in a mutant virus which escaped neutralization by soluble mCEACAM1$^a$[1,4] and which demonstrated decreased mCEACAM1$^a$[1,4] binding activity (43). Another substitution in the RBD, Q159L, was identified in several viruses isolated from persistently infected primary glial cell cultures; unlike the parental, wild-type MHV-A59, these mutant viruses were not hepatotropic (24). Thus, a single-amino-acid substitution in the RBD had dramatic effects on the outcome of infection.

Previous studies demonstrated that neutralization of MHV-4 requires threefold more smCEACAM1$^a$[1,4] than does neutralization of MHV-A59, while MHV-4 is not fully neutralized by 300-fold more smCEACAM1$^b$[1–4] than the amount required for complete neutralization of MHV-A59 (56). In the accompanying paper (55), we describe a liposome binding assay that was used to demonstrate that interaction of the receptor with spikes on virions at 37°C causes a conformational change that makes the virions sufficiently hydrophobic to bind to liposomes. (We use the word "triggered" to indicate that S undergoes a specific receptor-induced conformational change.) The availability of this assay and recombinant viruses expressing MHV-A59/MHV-4 chimeric spike proteins allowed us to define the functional domain(s) within the spike responsible for the receptor-induced conformational changes associated with viral entry.

We demonstrate here that in the comparison of recombinant viruses encoding chimeric MHV-A59/MHV-4 spike proteins in an in vitro liposome binding assay, the RBD of MHV-A59 is necessary and sufficient to allow triggering of spike to occur after incubation with either mCEACAM1$^b$[1–4] or mCEACAM1$^a$[1–4]. Furthermore, while the viruses expressing spikes with the RBD of either MHV-A59 or MHV-4 are able to infect BHK cells expressing mCEACAM1$^a$, the MHV-A59 RBD is generally necessary (with one exception, as described below) and sufficient to promote productive infection of BHK cells expressing mCEACAM1$^b$. These data demonstrate a role for the RBD in productive infection as well as in receptor discrimination.

## MATERIALS AND METHODS

**Cells and viruses.** Murine L2 and 17Cl-1 cells, feline FCWF cells, and baby hamster kidney (BHK) cells expressing CEACAM1$^a$[1–4] or CEACAM1$^b$[1,4] (15) were maintained on plastic tissue culture flasks in Dulbecco's minimal essential medium (DMEM; Gibco/BRL) with 10% fetal bovine serum (FBS; Gibco/BRL). Spinner cultures of L2 cells were maintained in Joklik's MEM with 10% FBS at densities of between $2 \times 10^5$ and $2 \times 10^6$ cells per ml. $S_{A59}$R13 and $S_{A59}$R14, are wild-type recombinant MHV-A59 isolates; since these viruses demonstrate no significant differences in phenotype in vitro or in vivo, they are collectively referred to as $S_{A59}$R. Likewise, $S_4$R21 and $S_4$R22, containing the MHV-4 spike in the MHV-A59 background, are be referred to as $S_4$R (39, 40). fMHV (obtained from P. Masters, New York State Department of Health, Albany, N.Y.) is a recombinant MHV strain which contains the ectodomain of the feline infectious peritonitis virus spike glycoprotein in place of that of the MHV-A59 spike (28).

**Recombinant proteins and antibodies.** Soluble murine CEACAM1$^a$ (smCEACAM1$^a$[1–4]) and CEACAM1$^b$ (smCEACAM1$^b$[1–4]) are the four-domain variant glycoproteins that are anchorless, six-histidine tagged, and produced by recombinant baculoviruses in Sf9 cells as described previously (56). AO4 is a goat antiserum directed against purified MHV-A59 spikes. It was detected by horseradish peroxidase (HRP)-conjugated rabbit anti-goat or swine anti-goat serum (Boehringer Mannheim). J7.2 and J7.18 are monoclonal antibodies directed against MHV-4 spike epitopes (obtained from J. Fleming, University of Wisconsin, Madison, Wis). J7.18 maps to S2 (9); there are conflicting data mapping J7.2 to S2 (34) and the hypervariable domain of S1 (38). Rabbit polyclonal antibodies 649 and 650 are directed against smCEACAM1$^a$[1–4] and smCEACAM1$^b$[1–4], respectively. Each antibody reacts with both mCEACAM1$^a$ and mCEACAM1$^b$ to a similar extent as measured by enzyme-linked immunosorbent assay (data not shown).

**Plasmids and mutagenesis.** PCR mutagenesis, using Vent polymerase (New England Biolabs) and the primers listed in Table 1, was used to construct the plasmids used in this study. The donor RNA transcription vectors were derived from pMH54 (obtained from P. Masters). pMH54 contains a T7 RNA polymerase promoter followed by a 9,139-nucleotide sequence (17, 28); pMH54 encodes the 5′ end of the MHV genome fused in frame to codon 28 of the hemagglutinin esterase (HE) pseudogene, followed by the spike and the rest of the 3′ end of the MHV-A59 genome and finally by a poly(A) tail. pGEM4Z, containing the MHV-4 spike gene, was obtained from M. J. Buchmeier, Scripps Institute, La Jolla, Calif.). Flanking *Avr*II and *Sse*8387I (Amersham; an isoschizomer of *Sbf*I) sites were introduced into the spike sequences near the 5′ and 3′ ends of the gene by the introduction of noncoding nucleotide changes, respectively, and the full start signal was added upstream of *Avr*II to create pG-MHV4S. pG-A59S was generated by inserting the *Avr*II-*Sse*8387I fragment of pMH54 into *Avr*II-*Sse*8387I cleaved pG-MHV4S.

To construct a plasmid which encodes a spike in which the RBD is derived from MHV-4 and the rest of the spike is derived from MHV-A59, the 5′-end 1,110 nucleotides of the MHV-4 S gene was amplified using JJ2 and RS366, flanking primers which also introduced unique *Avr*II and *Cla*I sites at the 5′ and 3′ ends, respectively. This amplified fragment was cleaved with *Avr*II and *Cla*I, sequenced, and subcloned into the corresponding region of the MHV-A59 spike gene in pG-A59S. The chimeric spike gene was excised with *Avr*II and *Sse*8387I and cloned into *Avr*II-*Sse*8387I-cleaved pMH54 to make the final donor RNA construct; this was called pMH54/MHV4S1N(370) since it is a modified pMH54, encoding a chimeric spike in which the amino-terminal 370 amino acids of S1 is from MHV-4 and the rest is from MHV-A59. To construct pMH54-S4/A59S1N(401), encoding a spike in which the amino-terminal 401 amino acids is derived from MHV-A59 and the rest is derived from MHV-4, the 5′-terminal 1,203 nucleotides of the MHV-A59 S gene was amplified using JFS1 and JRS414, flanking primers which also introduced unique *Avr*II and *Bsp*EI sites into the 5′ and 3′ ends of the fragment, respectively. This fragment was subcloned in place of the corresponding region of the MHV-4 spike gene in pG-MHV4S. The

TABLE 1. Primers used for PCR mutagenesis and genome sequencing

| Primer | Sequence (5′ to 3′)[a] | Sense | MHV-A59 spike gene location[b] |
|---|---|---|---|
| JJ2 | cgcgaagcttgaatccTAGGGTATATTGGTGATTTTAGATGTATCC | + | 36–73 |
| RS366 | GCGGAAGCatcgatATTATTACAAAACAAAGACTCAGCCTG | − | 1096–1134 |
| JFS1 | ATGCTGTTCGTGTTTATTCTA | + | 1–21 |
| JRS414 | GCGCAGTCTGCAGAAAtccggaGTTACCAATCTGTAAATC | − | 1204–1241 |
| SS2 | GTATCAATCTTATAATTAGC | − | 1240–1259 |
| A59-5 | AAGTGTATGGCAGGTGCTTTGG | + | 1136–1157 |
| WZL-60B | GAACATAGCTGCCGCAGTAGC | − | 2791–2811 |
| A59-9 | TCTGATGTTGGCTTTGTCGAGG | + | 2647–2668 |
| WZL-01 | GGGGGATCCAGGTAGC | − | Intergenic region between S and 4a open reading frame |

[a] Restriction sites introduced are denoted by lowercase letters.
[b] The locations are designated by nucleotide positions in the spike (S) open reading frame.

chimeric spike gene was cloned into pMH54-S4 to make pMH54-S4/A59S1N(401).

**Targeted RNA recombination.** The recombinant viruses expressing an MHV-A59 spike in which the N terminus was replaced with MHV-4 spike sequences are called $S_{A59}(N_4)$ viruses. They were selected using a modification of published techniques (25, 40). Recombination was carried out in L2 cells between capped donor RNA molecules, transcribed from *Pac*I-linearized pMH54/MHV4S1N (370), and the recipient virus, $S_4$R21, which expresses the wild-type MHV-4 spike (40). Infected or transfected L2 cells were plated onto 17Cl-1 cells, and the culture medium, containing the progeny recombinant viruses, was collected. To eliminate $S_4$R21 and other viruses encoding larger regions of the MHV-4 spike gene, the released viruses were incubated with anti-MHV-4 spike antibodies J7.2 and J7.18 for 1 h at 4°C and plaque purified on L2 cells. The antibody-resistant recombinants were analyzed by restriction digestion to identify viruses with chimeric spike proteins. The desired recombinants were plaque purified on L2 cells once more, and two viruses from independent recombination events were chosen for study and named $S_{A59}(N_4)$R31 and $S_{A59}(N_4)$R33. Viruses that express an MHV-4 spike in which the N terminus has been replaced by MHV-A59 spike sequences are called $S_4(N_{A59})$ viruses. Generation of these viruses used a further modified technique (28, 39). Recombination was carried out in feline FCWF cells between the donor RNA [transcribed from pMH54-S4/A59S1N(401)] and the recipient virus, fMHV. The recombinant viruses were selected by two rounds of plaque purification on L2 cells. Two $S_4(N_{A59})$ viruses from independent recombination events were chosen for study and were named $S_4(N_{A59})$R61 and $S_4(N_{A59})$R62.

**Spike gene analysis.** Intracellular RNA from infected cells was used to amplify cDNA (31, 40), which was sequenced using the *Taq* dye terminator procedure as specified by the manufacturer (Taq DyeDeoxy terminator cycle-sequencing kit; Applied Biosystems). All recombinant MHV spike genes were sequenced in full using primers listed in Table 1 and described previously (31, 40) and were compared to our laboratory MHV-A59 spike (24) or MHV-4 spike (38) gene sequences. Our wild-type MHV-4 spike gene has, compared to the published sequence, one silent mutation at nucleotide 3990 and an L255A substitution (40). The $S_{A59}(N_4)$R31 spike glycoprotein contained the N-terminal 371 amino acid residues of the MHV-4 sequence in the MHV-A59 spike and a secondary mutation, I998L. The $S_{A59}(N_4)$R33 spike had 462 amino acid residues of MHV-4 at the N terminus of the MHV-A59 spike and no secondary mutations. $S_4(N_{A59})$R61 and $S_4(N_{A59})$R62 each contained 401 amino acid residues of MHV-A59 sequence, replacing the equivalent region in the N terminus of the MHV-4 spike glycoprotein; each recombinant virus had a secondary mutation, L620I and L1114F, respectively.

**Virus purification.** Virus stocks were prepared in infected 17Cl-1 cells. Virus particles were precipitated in a 30% polyethylene glycol (average molecular weight 8,000; Sigma) saline solution. The pellet was resuspended in 25 mM BisTris saline (pH 6.5) and purified through a 20%/50% sucrose step gradient in an SW28 (Beckman) rotor at 83,000 × *g* for 4 h at 4°C. The virus band at the 20%/50% sucrose interface was collected, diluted with BisTris saline, and further purified through a 20 to 50% continuous sucrose gradient in the SW28 rotor at 83,000 × *g* for 18 h at 4°C. Virus, recovered as a visible band, was dialyzed (tubing with a molecular weight cutoff of 12,000 to 14,000; Spectrum) for 18 h at 4°C against 25 mM BisTris (pH 6.5)–150 mM NaCl–5% glycerol, flash frozen in aliquots, and stored at −80°C.

**Thermal and pH inactivation.** Approximately equal amounts of viruses (as estimated by staining with AO4 antiserum on Western blots, corresponding to $10^5$ to $10^6$ PFU) were diluted into DMEM with 10% fetal bovine serum and then incubated at 42°C in an equal volume of 2X TMEN (100 mM Tris maleate [pH 6.5], 2mM EDTA, 400 mM NaCl) with 10% fetal bovine serum adjusted to pH 8.6. Samples were frozen at each time point and subsequently subjected to titer determination by plaque assay on L2 cells.

**Liposome-flotation assay.** Purified virus was incubated with 0.9 μM smCEACAM1$^a$[1–4] or smCEACAM1$^b$[1–4] and an equal volume of liposomes in a final volume of 100 or 150 μl of BisTris saline at 37°C for 30 min. (Approximately equal amounts of protein for each purified virus, as estimated by staining with AO4 antiserum on Western blots, equivalent to the amount in $10^6$ PFU of $S_{A59}$R, were used in the assay.) The liposomes were composed of phosphatidylcholine, phosphatidylethanolamine, and cholesterol in a 1:1:1 molar ratio and prepared as described in the accompanying paper (55). The reaction was terminated on ice, and the reaction mixture was mixed with 62% sucrose solution to make a 50% sucrose solution. (The sucrose solutions were made in 25 mM BisTris–150 mM NaCl [pH 6.5].) The sucrose gradient was constructed of layered 10, 20, 30, and 40% sucrose solutions in a 5-ml Ultra-Clear centrifuge tube (Beckman), assembled the night before and stored at 4°C. The gradient, with the reaction mix at the bottom, was centrifuged in an SW-55 Ti (Beckman) for 2.5 h at 59,000 × *g* and 4°C and subsequently fractionated using a peristaltic pump from the air/liquid interface. Aliquots of the fractions were blotted onto polyvinylidene difluoride membranes (Millipore). The blots were probed with antiserum AO4 for MHV spike, and the secondary antibody, HRP-conjugated rabbit anti-goat was detected by chemiluminescence as instructed by the manufacturer (Amersham).

**Viral growth curves.** Confluent monolayers of L2 and BHK cells expressing mCEACAM1$^a$[1–4] or mCEACAM1$^b$[1,4] were infected in duplicate or triplicate with viruses at a multiplicity of infection (MOI) of 2 PFU/cell at 4°C for 1 h. The inocula were removed, and the cells were washed with phosphate-buffered saline (PBS). After fresh medium was added, the plates were incubated at 37°C. At the indicated time points after infection, the plates were transferred to −80°C and freeze-thawed twice; lysates were clarified and subjected to titer determination for PFU on L2 cells (22). The surface expression level of mCEACAM1$^a$ and mCEACAM1$^b$ in BHK cells expressing each protein was monitored by flow cytometry using polyclonal antibody 649 or 650. Murine CEACAM1$^a$ expression was found on 20% of the cells, and its level as measured by the geometric mean fluorescence intensity was within twofold of the geometric mean fluorescence of mCEACAM1$^b$, which was expressed on 30% of the cells (data not shown).

**Formation of mCEACAM-independent syncytia.** Monolayers of L2 cells were infected with viruses at MOI of 2 PFU/cell or mock infected at 37°C for 2 h. The inocula were removed, and the cells were washed with PBS. The cells were dissociated with trypsin-EDTA (GIBCO-BRL) and diluted with 10% FBS-containing medium. L2 cells were added to confluent monolayers of BHK cells in a 1:10 ratio to minimize cell-to-cell fusion among L2 cells. The same number of L2 cells was added to empty wells as a negative control. Additional fresh medium was added to the plates, which were then incubated at 37°C. The BHK monolayers were examined for syncytium formation 20 to 24 h after infection. The cells were visualized under phase-contrast microscopy after fixation with 2% paraformaldehyde in PBS.

## RESULTS

**Selection of recombinants differing in the RBD of the spike protein.** We have previously selected and characterized isogenic recombinant MHV strains differing only in the spike

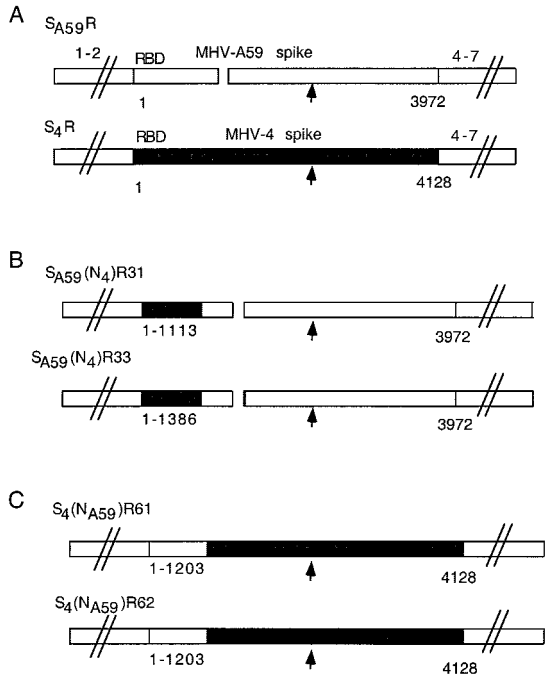


FIG. 1. Recombinant viruses expressing parental and chimeric MHV-A59/MHV-4 spike glycoproteins. The genomes of recombinant viruses expressing either wild-type MHV-A59 or MHV-4 spike genes or chimeric MHV-A59/MHV-4 spike genes are shown. The background genes (designated 1–2 and 4–7) of all recombinant viruses are derived from MHV-A59. The 5′-terminal region of the spike gene is designated RBD (approximately 330 amino acids). The arrow designates the site of cleavage, the boundary between S1 and S2. (A) The $S_{A59}R$ and $S_4R$ viruses contain the full-length wild-type MHV-A59 and MHV-4 spike glycoproteins, respectively (solid bar, MHV-4 sequence of 4,128 nucleotides [encoding 1,376 amino acids]; open bar, MHV-A59 sequence of 3,972 nucleotides [encoding 1,324 amino acids]). The break in the MHV-A59 spike represents a 52-amino-acid in-frame deletion relative to the MHV-4 spike (38). (B) Viruses expressing chimeric spike with the RBD from MHV-4 and the rest of the spike from MHV-A59 include $S_{A59}(N_4)R31$ and $S_{A59}(N_4)R33$. These viruses contain 1,113 and 1,386 nucleotides (encoding 371 and 462 amino acids), respectively, from the 5′ end of the MHV-4 spike gene. (C) Viruses expressing chimeric spike with the MHV-A59 RBD and the rest from MHV-4 include $S_4(N_{A59})R61$ and $S_4(N_{A59})R62$. These viruses each contain 1,203 nucleotides (encoding 401 amino acids) from the 5′ end of the MHV-A59 spike gene.

gene (40). These viruses express either the MHV-A59 spike ($S_{A59}R$) or the MHV-4 spike ($S_4R$), with the rest of the viral genes derived from MHV-A59 (Fig. 1). More recently, to study the effects of the RBD on MHV infection, we selected groups of recombinant viruses encoding either the MHV-A59 or MHV-4 spike proteins in which the RBDs of MHV-4 and MHV-A59 were exchanged (Fig. 1); we then compared these viruses to parental $S_4R$ and $S_{A59}R$ viruses for their ability to use the viral receptors mCEACAM1[a] and mCEACAM1[b].

Viruses expressing chimeric spike proteins with the MHV-4 RBD and the rest of the spike derived from MHV-A59 were generated using targeted RNA recombination with an RNA containing the 5′ 1,110 nucleotides (370 codons) from the MHV-4 spike gene, as described in Materials and Methods. This involved using $S_4R$, a recombinant with a full-length MHV-4 spike gene, as the parental virus and selecting against the parent by using two spike monoclonal antibodies mapping outside of the RBD. Interestingly, most of the recombinants selected (18 of 19 examined from two independent recombination events) contained larger regions of MHV-4 sequence, 1,386 nucleotides (462 codons) or more (Fig. 1). Only one of these recombinants had an MHV-4 sequence length close to that of the input RNA; this virus, $S_{A59}(N_4)R31$, had 1,113 nucleotides (371 codons) of the MHV-4 spike sequences and was chosen for further analysis. One of the recombinants with the longer MHV-4 sequence, $S_{A59}(N_4)R33$, with 1,386 5′ nucleotides derived from the MHV-4 spike, was also analyzed further. The low frequency of viruses with the input MHV-4 5′ sequence suggests that there may be some selective advantage in vitro for viruses with longer N-terminal sequence derived from MHV-4. We also placed the MHV-A59 RBD in the corresponding region of the MHV-4 spike by using a donor RNA with the 5′ 1,203 nucleotides (401 codons) of the spike gene derived from MHV-A59 (Fig. 1). In this case, since the parental virus expressed the feline coronavirus spike gene (see Materials and Methods), the selection for replication on murine cells required the entire murine spike to replace the feline infectious peritonitis virus spike gene; thus, all recombinants examined had the same spike sequence as the donor RNA, that is, 1,203 nucleotides of MHV-A59 sequence. Two of these, $S_4(N_{A59})R61$ and $S_4(N_{A59})R62$, were chosen for further analysis.

We measured the in vitro fitness of the recombinant viruses, expressing either MHV-A59 or MHV-4 spike proteins or chimeric spike proteins, by generating one-step growth curves with murine L2 fibroblasts (Fig. 2). As observed previously, $S_4R$ viruses replicate to titers approximately 100-fold lower than $S_{A59}R$ viruses (40). This is similar to the difference in replication in vitro between parental MHV-4 and MHV-A59 strains (40). All of the viruses expressing chimeric spikes replicated efficiently in vitro, to titers significantly greater than that of $S_4R$ and close to that of $S_{A59}R$. Interestingly, $S_{A59}(N_4)R31$, the virus with the shortest MHV-4 sequence in the chimeric spike glycoprotein, formed fuzzy plaques, unlike the clear plaques with well-defined borders formed by $S_{A59}R$ and $S_4R$. The other chimeric viruses formed plaques of sizes that were intermediate between the plaque sizes of $S_{A59}R$ (3 mm) and $S_4R$ (1 mm) when visualized 24 h after infection.

These viruses were compared for the rate of inactivation when subjected to elevated temperature (42°C) and pH (pH 8.6), as shown in Fig. 3. The recombinant viruses expressing wild-type MHV-4 and MHV-A59 spikes were more labile than the viruses expressing chimeric spike proteins. Furthermore, $S_4R$ was more labile than $S_{A59}R$; this probably reflects previous observations that the MHV-4 spike more readily loses the S1 subunit when incubated with soluble receptor in a neutralization assay (18). Thus, the data in Fig. 3 demonstrate that lability is not associated with either the RBD or the C-terminal portions of the spike but, rather, results from a combination of the two portions of the spike.

**The RBD of the spike proteins determines the ability to trigger conformational change in response to soluble mCEACAM1[a] and mCEACAM1[b] in a liposome binding assay.** Viral entry at the plasma membrane relies on the binding of a viral envelope protein to a host receptor, which triggers a conformational change in the envelope protein, leading to

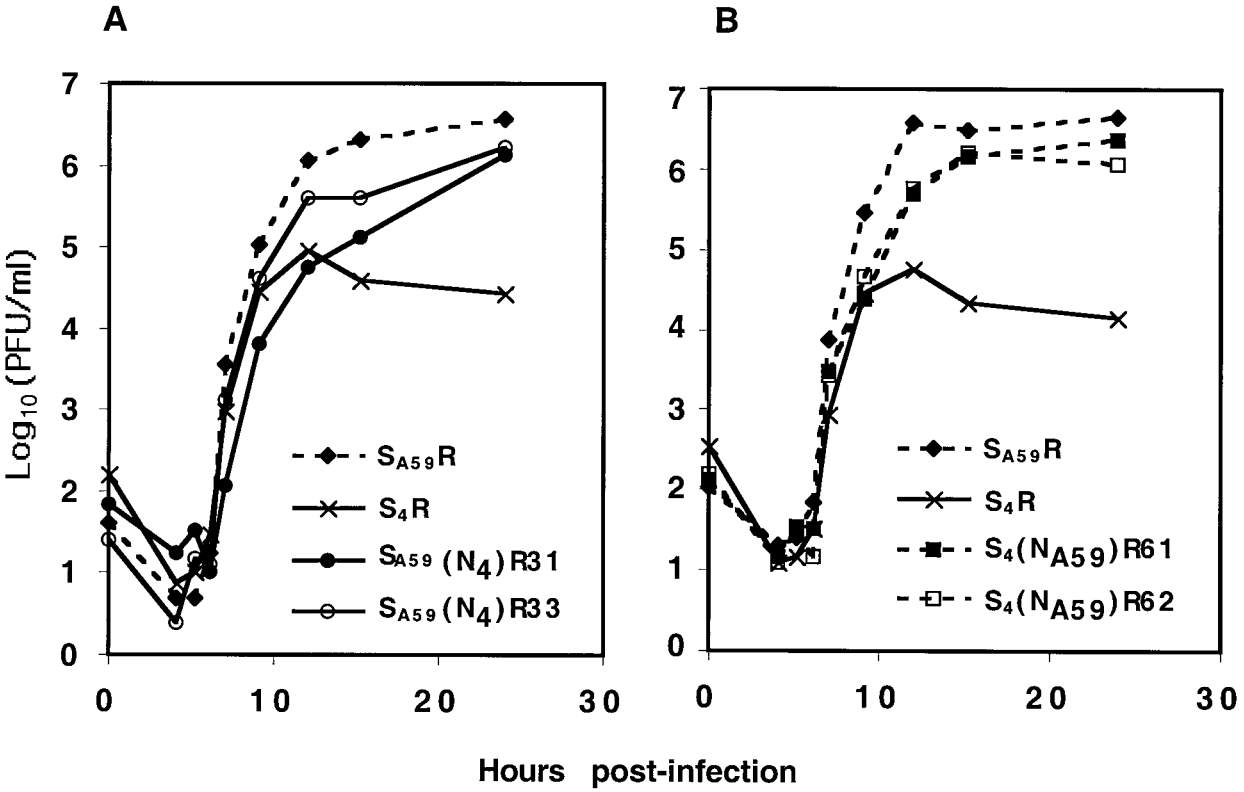


FIG. 2. Replication of recombinant viruses in L2 cells. One-step growth curves for recombinant viruses expressing wild-type and chimeric spikes were generated in experiments with L2 cells with an MOI of 2 PFU/cell and in duplicate wells, as described in Materials and Methods. The $S_4R$ and $S_{A59}R$ viruses in panels A and B are independently selected viruses with wild-type spike proteins. Curves for viruses with spikes containing the MHV-4 RBD are indicated by solid lines, while viruses with spikes containing the MHV-A59 RBD are indicated by dotted lines.

fusion of the viral and cell membranes (13). Previous studies with retroviruses, using a liposome flotation assay, have demonstrated the activation of soluble viral envelope glycoprotein by soluble receptor glycoproteins and the subsequent association of the viral glycoprotein with target membranes (8, 23). We have used a similar liposome association assay (described in the accompanying paper [55]) to test the hypotheses that the ability of murine coronavirus virions to associate with liposomes depends on the interaction between the spike protein and the mCEACAM glycoprotein and that the ability to utilize mCEACAM1$^a$ and/or mCEACAM1$^b$ depends on the RBD of the viral S protein. We performed the liposome flotation assay by incubating purified virus with soluble mCEACAM1 glycoproteins and determined whether the virus colocalized with liposomes after centrifugation in a sucrose density gradient. Virus that associates with liposomes would "float" up under these conditions and be located in the lower-density portions of the gradient.

At 4°C, without liposomes or without soluble mCEACAM, all viruses remained at the bottom of the gradient following centrifugation (data not shown). Figure 4A shows that incubation with smCEACAM1$^a$[1–4] at 37°C for 30 min shifted $S_{A59}R$ to lower-density (top) fractions of the gradients. In contrast, the addition of smCEACAM1$^a$[1–4] at 37°C for 30 min caused only a small shift of $S_4R$ to lower-density following sedimentation (Fig. 4A). The recombinant viruses expressing chimeric spike proteins, $S_{A59}(N_4)R31$ and $S_{A59}(N_4)R33$ (expressing the MHV-4 RBD [Fig. 4B]) as well as $S_4(N_{A59})R61$ (expressing the MHV-A59 RBD [Fig. 4C]), also associated with liposomes after interacting with smCEACAM1$^a$ at 37°C and pH 6.5. This observation suggests that spike proteins, containing either the MHV-A59 or MHV-4 RBD on virions, are capable of undergoing a conformational change induced by smCEACAM1$^a$, even when expressed in chimeric spike glycoproteins.

In the presence of smCEACAM1$^b$ after treatment at 37°C for 30 min, $S_{A59}R$ moved with the liposomes to the lower-density fractions (Fig. 4A). In contrast, viruses expressing either wild-type MHV-4 spike ($S_4R$) or chimeric spikes with the MHV-4 RBD [$S_{A59}(N_4)R31$ and $S_{A59}(N_4)R33$] remained at the bottom after incubation at 37C with smCEACAM1$^b$. These data suggest that the MHV-4 RBD was impaired in its interaction with smCEACAM1$^b$ and that the MHV-A59 RBD was necessary for the use of smCEACAM1$^b$. This is in agreement with previous observations that MHV-4 was not efficiently neutralized by smCEACAM1$^b$ (56).

The observation that $S_4(N_{A59})R61$ associated with liposomes after incubation with either smCEACAM1$^a$ or smCEACAM1$^b$ (Fig. 4C), as did $S_{A59}R$, demonstrates that the MHV-A59 RBD was sufficient for efficient interaction with smCEACAM1$^b$ even when the rest of the spike was from MHV-4. Thus, the recombinant virus containing the MHV-A59 RBD (with the rest of the spike from MHV-4) was triggered by either smCEACAM1$^a$ or smCEACAM1$^b$, promoting

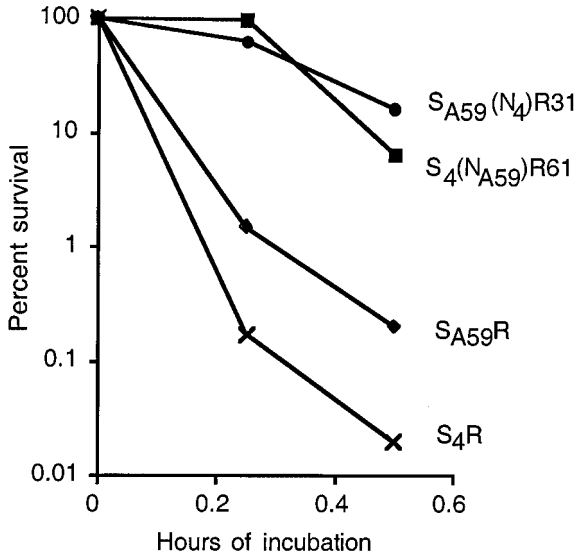


FIG. 3. Viral inactivation. Recombinant viruses $S_{A59}R$, $S_4R$, $S_{A59}(N_4)R31$, and $S_4(N_{A59})R61$, as indicated, were incubated at 42°C and pH 8.6 for the times indicated. Infectious virus was then subjected to titer determination by a plaque assay on L2 cells.

association with liposomes; this is in contrast to the recombinants containing the MHV-4 RBD (with the rest of the spike from MHV-A59), which were associated with liposomes after incubation with smCEACAM1$^a$ but not with smCEACAM1$^b$.

**The RBD determines the ability of the virus to replicate in BHK cells expressing membrane-anchored mCEACAM1$^a$ or mCEACAM1$^b$.** To determine whether our observations of differences in mCEACAM utilization in the triggering of spike protein that promote lipid association in the liposome flotation assay do indeed reflect functional differences in cell entry, one-step curves similar to those shown in Fig. 2 were generated in experiments using BHK cells stably transfected with cDNA encoding either mCEACAM1$^a$ or mCEACAM1$^b$ glycoproteins; these cells are called BHK-mCEACAM1$^a$[1–4] or BHK-mCEACAM1$^b$[1,4], respectively (Fig. 5).

Both wild-type and chimeric spike-expressing viruses replicated in BHK-mCEACAM1$^a$ cells with slower kinetics than but to similar final titers as in L2 cells, which express CEACAM1$^a$ (compare Fig. 2 with Fig. 5A). As in L2 cells, $S_4R$ replicated in BHK-mCEACAM1$^a$ cells significantly less efficiently than did $S_{A59}R$, and all of the chimeric spike viruses were similar, but perhaps slightly less efficient than $S_{A59}R$ in replication. In BHK-mCEACAM1$^b$ cells, however, replication of all viruses was considerably slower and the final titers attained were much lower than those observed in either L2 cells or BHK-mCEACAM1$^a$ cells (Fig. 2 and 5). Most strikingly, recombinant viruses expressing MHV-4 RBD [$S_{A59}(N_4)R31$ and $S_{A59}(N_4)R33$] did not replicate in BHK-mCEACAM1$^b$ cells, even at late time points (Fig. 5B). In contrast, recombinant viruses expressing the MHV-A59 RBD in the background of the MHV-4 spike [$S_4(N_{A59})R61$ and $S_4(N_{A59})R62$] replicated in BHK-mCEACAM1$^b$ cells significantly better did than $S_{A59}(N_4)R31$ and $S_{A59}(N_4)R33$ (Wilcoxon's rank sum test, $P < 0.03$). Thus, as in the in vitro liposome association assay, the chimeric recombinant viruses with the MHV-A59 RBD can use sCEACAM1$^b$ more efficiently to mediate an infection in cultured cells than those with MHV-4 RBD.

In contrast to $S_{A59}(N_4)R31$ and $S_{A59}(N_4)R33$ (containing the MHV-4 RBD), in BHK-mCEACAM1$^b$ cells $S_4R$ virus attained titers similar to those of the MHV-A59 RBD-containing chimeric viruses. This may seem surprising in light of the inability of the viruses expressing spike with the MHV-4 RBD, including $S_4R$, to utilize smCEACAM1$^b$, as demonstrated by the liposome association assay. We reasoned that the ability to replicate in BHK-mCEACAM1$^b$ cells was probably due to the ability of the MHV-4 spike to mediate mCEACAM1-independent cell-to-cell fusion (20). While hamster cells cannot be infected by either MHV-A59 or MHV-4 virions, cell-to-cell spread of virus infection can occur from mouse cells infected with MHV-4 into hamster cells that do not express mCEACAM1. This would allow the spread of virus from BHK

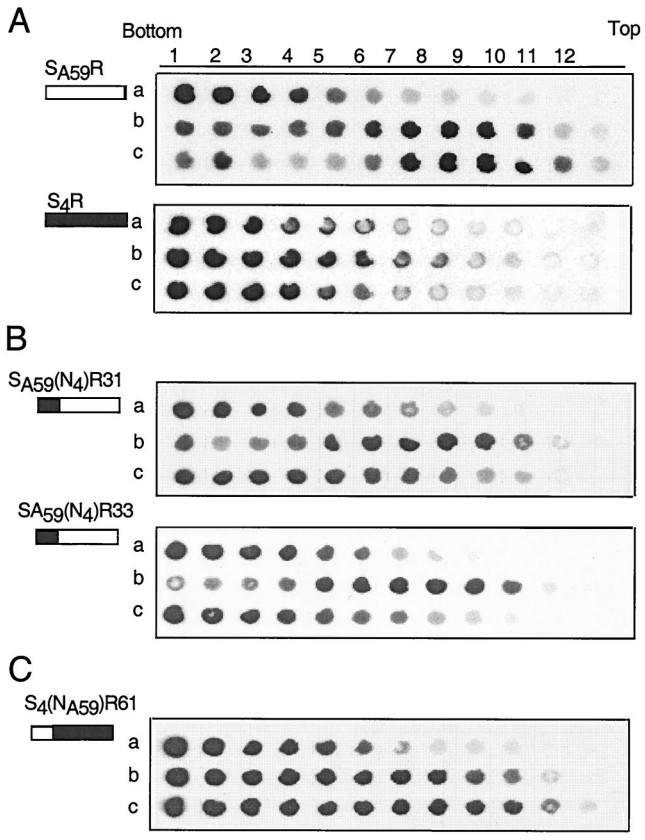


FIG. 4. The association of recombinant viruses with liposomes depends on soluble mCEACAM1$^a$ and mCEACAM1$^b$. Viruses were incubated with liposomes alone (row a), with smCEACAM1$^a$ (row b), or with smCEACAM1$^b$ (row c) at 37°C for 30 min; the reaction mixtures were centrifuged through 10 to 50% sucrose density gradients. Samples from individual fractions (numbered from bottom to top) were blotted onto polyvinylidene difluoride membranes and incubated with anti-spike AO4 antibody. The small diagrams to the left of each blot represent the spike proteins; the solid areas represent MHV-4 sequences, and the open areas represent MHV-A59 sequences. (A) Viruses expressing parental wild-type spikes, $S_{A59}R$ and $S_4R$; (B) viruses expressing chimeric spikes with the MHV-4 RBD, $S_{A59}(N_4)R31$ and $S_{A59}(N_4)R33$; (C) virus expressing a chimeric spike with the MHV-A59 RBD, $S_4(N_{A59})R61$.

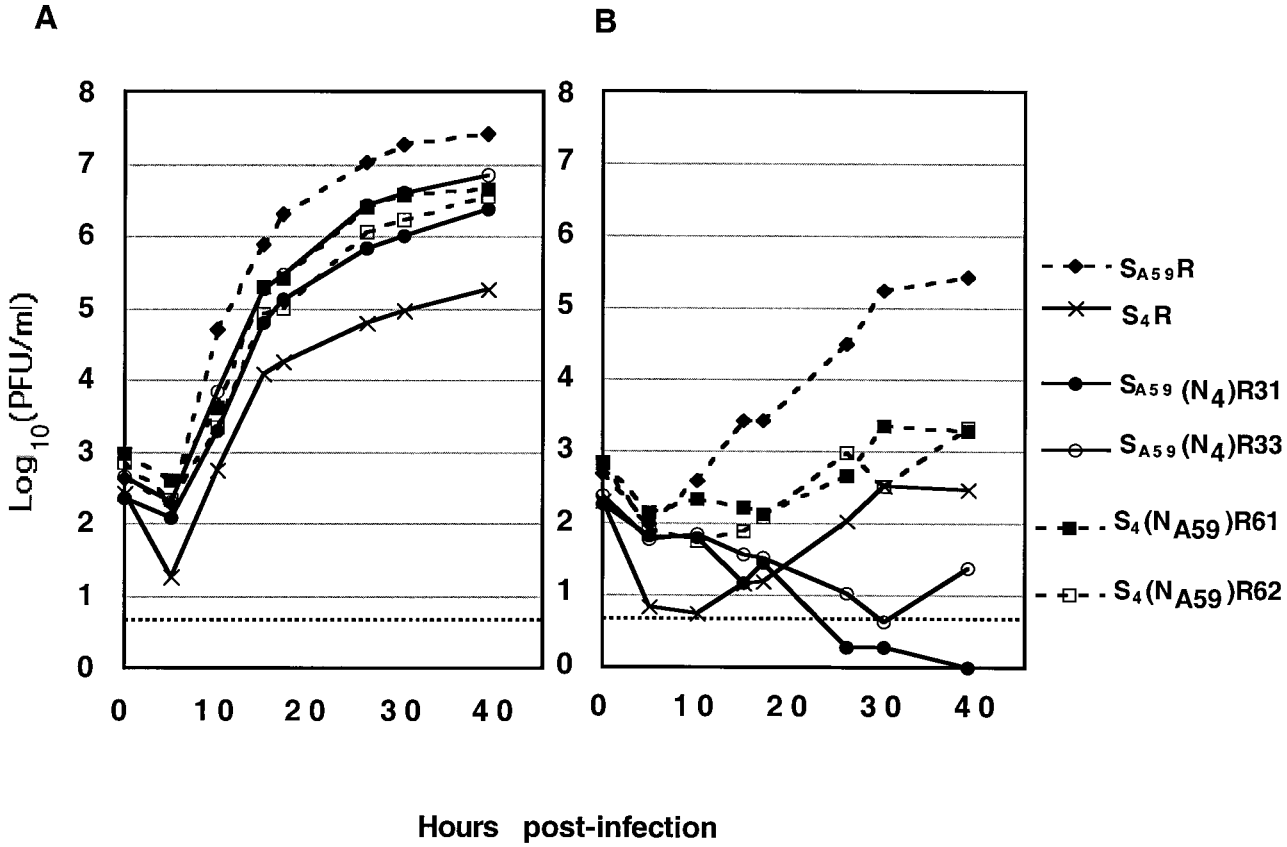


FIG. 5. Growth kinetics of recombinant viruses in BHK cells expressing mCEACAM1[a] or mCEACAM1[b]. One-step growth curves (MOI = 2 PFU/cell) were generated for BHK-mCEACAM1[a][1–4] (A) or BHK-mCEACAM1[b][1,4] (B) cells as described in Materials and Methods. For each virus, replication is expressed as the logarithmic mean titer of 5 independently infected wells pooled from two separate experiments. At 39 h postinfection, the replication of $S_4(N_{A59})$R61 and $S_4(N_{A59})$R62 was significantly greater than that of $S_{A59}(N_4)$R31 and $S_{A59}(N_4)$R33 (Wilcoxon's rank sum test; $P < 0.03$).

cells expressing mCEACAM1[b] to BHK cells even if the initial infection using CEACAM1[b] receptor were inefficient.

To determine if CEACAM-independent spread was the explanation for the ability of $S_4$R to replicate in BHK-mCEACAM1[b] cells, we investigated the ability of the recombinant viruses to carry out mCEACAM1-independent fusion. Thus, L2 cells were infected with viruses expressing either wild-type or chimeric spike proteins and then plated in a 1:10 ratio onto a monolayer of nonpermissive BHK cells. After 20 h, large syncytia were observed in the $S_4$R-infected cells but not in cells infected with either $S_{A59}(N_4)$R31 or $S_4(N_{A59})$R61 (Fig. 6). (Similarly, recombinant viruses expressing the other chimeric spikes were unable to induce fusion of BHK monolayers [data not shown].) The low ratio of L2 to BHK cells was used to minimize the likelihood of L2 cells fusing among themselves. Indeed the fusion observed could not be among L2 cells alone because only a few small syncytia were observed among L2 cells plated alone in wells without BHK monolayers (data not shown). Thus, of all the viruses tested, only $S_4$R has the ability to spread from cell to cell in the absence of the mCEACAM1 viral receptor. This probably explains our observation that $S_4$R replicates in cells expressing mCEACAM1[b], which is generally a poor receptor for viruses containing the RBD of MHV-4.

## DISCUSSION

We have examined the RBD of the spike within viruses by generating otherwise isogenic recombinant viruses expressing chimeric MHV-4/MHV-A59 spike glycoproteins. Studying recombinant viruses rather than biologically selected variant viruses, used in previous studies of virus-receptor interaction, offers the advantages of isogenic background and the ability to identify the RBD as a major determinant in using different mCEACAM glycoproteins. We have used two assays to examine the role of RBD in infection, an in vitro liposome association assay and the replication of virus in vivo in BHK cells that express either mCEACAM1[a] or mCEACAM1[b]. The results of both assays suggest that while spike proteins with the MHV-A59 RBD can utilize either mCEACAM1[a] or mCEACAM1[b], spike proteins with the RBD derived from MHV-4 cannot efficiently use mCEACAM1[b]. Our data are in agreement with a previous report that while smCEACAM1[a] neutralizes the infectivity of MHV-A59 and MHV-4 (JHM), smCEACAM1[b] can effectively neutralize MHV-A59 but not MHV-4 (56).

Viruses expressing spike protein with RBD derived from either MHV-A59 or MHV-4, whether wild type or chimeric, colocalized with liposomes in the presence of smCEACAM1[a] after incubation at 37°C for 30 min at pH 6.5; in contrast, only

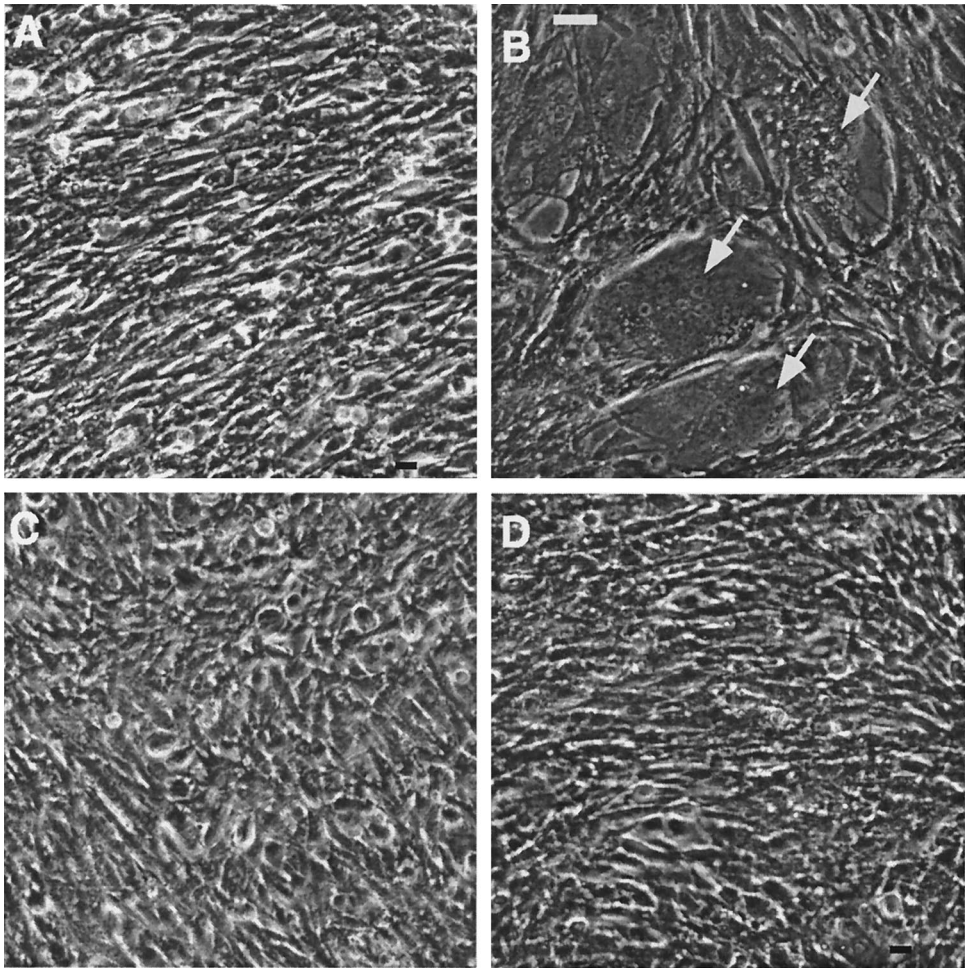


FIG. 6. $S_4$R-infected L2 cells form CEACAM-independent syncytia with BHK cells. Infected L2 cells were dissociated and added to monolayers of uninfected BHK cells at a 1:10 ratio. After 20 h, the cells were fixed and visualized by phase-contrast microscopy at 200× magnification. (A) $S_{A59}$R. (B) $S_4$R. (C) $S_{A59}(N_4)$R31. (D) $S_4(N_{A59})$R61. The arrows indicate several large syncytia. Bar, 40 μm.

viruses with the MHV-A59 RBD used smCEACAM1[b] efficiently, as assayed by liposome association. One exception to this general conclusion was that incubation with smCEACAM1[a] facilitated the association of $S_4$R with liposomes quite inefficiently (Fig. 4). There are possible explanations for this, related to the fact that this assay measures total virions rather than infectious particles. $S_4$R (like wild-type MHV-4) virions have a significantly higher protein-to-PFU ratio (as estimated by Western blotting) than do the other viruses; the ratio of protein to PFU for $S_4$R virions is about 100-fold higher than that for $S_{A59}$R (data not shown). Therefore, it is likely that a large fraction of MHV-4 particles are inactivated prior to the assay and only a small fraction of the virus particles or spikes are competent for association with liposomes. Indeed, it has been shown that the MHV-4 spike protein is less stable in terms of S1–S2 association and more easily becomes fusion competent than other MHVs, sometimes without receptor (18, 26). Consistent with this, $S_4$R is more labile when heated to 42°C at pH 8.6 than are the other recombinant viruses (Fig. 3).

We also examined the role of the RBD in determining the able to utilize anchored receptor glycoproteins in MHV infection. We carried out growth curves in BHK cells expressing either anchored mCEACAM1[a] or mCEACAM1[b] (Fig. 5). All of the viruses expressing either wild-type or chimeric spikes were able to use mCEACAM1[a] to replicate efficiently and to similar titers to those in in L2 cells, which also express mCEACAM1[a] (compare Fig. 2 and 5). The patterns of replication in CEACAM1[b] cells were, however, quite different. None of the viruses was able to replicate nearly as efficiently as in mCEACAM1[a]-expressing cells. Even $S_{A59}$R, which expresses the wild-type MHV-A59 spike, replicated to a final titer of approximately 100-fold less than in mCEACAM1[a] expressing cells. All viruses expressing spike proteins with the MHV-A59 RBD [full-length $S_{A59}$R or chimeric $S_4(N_{A59})$R61 and $S_4(N_{A59})$R62] replicated in mCEACAM1[b] cells, while the viruses expressing chimeric spikes with the MHV-4 RBD [$S_{A59}(N_4)$R31 and $S_{A59}(N_4)$R33] replicated very poorly, if at all. Thus, consistent with the in vitro liposome association assay, the ability to utilize mCEACAM1[b] to mediate a productive infection in BHK cells is determined by the presence of the MHV-A59 RBD.

The pattern of replication of the virus expressing full-length

MHV-4 spike ($S_4R$) was markedly different, in BHK cells expressing mCEACAM1$^b$, from that of $S_{A59}(N_4)R31$ and $S_{A59}(N_4)R33$, in that $S_4R$ replicated to a significant degree. This was probably because mCEACAM-independent fusion contributed to the spread of infection from cell to cell. As has been demonstrated previously (20, 26), infection with viruses expressing the full-length MHV-4 spike protein can induce cell-to-cell fusion in an mCEACAM-independent process. Consistent with this, $S_4R$ is the only virus studied here that can mediate mCEACAM-independent cell-to-cell fusion (Fig. 6). Thus, it is likely that once $S_4R$ enters the BHK-mCEACAM1$^b$ cells, probably inefficiently via the mCEACAM1$^b$ receptor, it can spread from cell to cell in the absence of receptor. This would explain the increased ability of $S_4R$ to replicate in mCEACAM1$^b$-expressing BHK cells compared to the viruses expressing chimeric spikes with the MHV-4 RBD.

While we have shown that the RBD plays a role in determining the ability to utilize mCEACAM1$^b$, it is also clear that other portions of the spike also play a role in the structure of the spike-receptor interaction and in the early steps of viral entry. Evidence for this is provided by the observation that $S_4R$ is the only recombinant virus analyzed here (as well as other viruses expressing MHV-4 spikes with deletions within S1 [data not shown]) that has the ability to carry out receptor-independent cell fusion (Fig. 6). This is probably the explanation for why $S_4R$ can replicate in BHK cells expressing mCEACAM1$^b$ while other viruses expressing chimeric spike proteins with the MHV-4 RBD cannot replicate in these cells (Fig. 6). $S_4R$ also is less efficient than other viruses expressing spikes with the $S_4R$ RBD [$S_{A59}(N_4)R31$ and $S_{A59}(N_4)R33$] at undergoing conformational change after incubation at 37°C with smCEACAM1$^a$ (Fig. 4) and also is inefficient at replication in vitro (Fig. 2 and 5). These data are consistent with results of earlier studies, which showed that the MHV-4 spike glycoprotein is more susceptible to irreversible conformational changes than is the MHV-A59 spike, and with our observation that $S_4R$ was also more labile in the presence of elevated temperature and pH than were the other recombinant viruses (Fig. 3). This is also in agreement with previous data on the relationship of lability and receptor-independent fusion (20). It is not clear whether this is related to any of these other differences among viruses expressing wild-type or chimeric spikes (18, 26). Thus, these data indicate that these properties, unique to $S_4R$ (and parental MHV-4), are associated not with the RBD alone but with more downstream domains as well. The MHV-4 spike has evolved to optimize infection and spread of virus within the mouse. It is likely that the RBD and the rest of the spike must coevolve to optimize the ability of the spike to function in early virus-cell interactions, which lead to viral entry, and in later interactions which promote cell-to-cell spread.

## ACKNOWLEDGMENTS

This work was supported by Public Health Service grants NS-21954 and NS-30606 to S.R.W. and AI-25231 to K.V.H. J.C.T. was supported in part by funds from grant NIH-T32-AI-07325.

## REFERENCES

1. **Baric, R. S., E. Sullivan, L. Hensley, B. Yount, and W. Chen.** 1999. Persistent infection promotes cross-species transmissibility of mouse hepatitis virus. J. Virol. **73:**638–649.
2. **Baric, R. S., B. Yount, L. Hensley, S. A. Peel, and W. Chen.** 1997. Episodic evolution mediates interspecies transfer of a murine coronavirus. J. Virol. **71:**1946–1955.
3. **Beauchemin, N., T. Chen, P. Draber, G. Dveksler, P. Gold, S. Gray-Owen, F. Grunert, S. Hammarstrom, K. V. Holmes, A. Karlsson, M. Kuroki, S. H. Lin, L. Lucka, S. M. Najjar, M. Neumaier, B. Obrink, J. E. Shively, K. M. Skubitz, C. P. Stanners, P. Thomas, J. A. Thompson, M. Virji, S. von Kleist, C. Wagener, S. Watt, and W. Zimmermann.** 1999. Redefined nomenclature for members of the carcinoembryonic antigen family. Exp. Cell Res. **252:** 243–249.
4. **Boyle, J. F., D. G. Weismiller, and K. V. Holmes.** 1987. Genetic resistance to mouse hepatitis virus correlates with absence of virus-binding activity on target tissues. J. Virol. **61:**185–189.
5. **Cavanagh, D.** 1995. The coronavirus surface glycoprotein, p. 73–113. *In* S. G. Siddell (ed.), The *Coronaviridae.* Plenum Press, New York, N.Y.
6. **Chen, D. S., M. Asanaka, F. S. Chen, J. E. Shively, and M. M. Lai.** 1997. Human carcinoembryonic antigen and biliary glycoprotein can serve as mouse hepatitis virus receptors. J. Virol. **71:**1688–1691.
7. **Compton, S. R., C. B. Stephensen, S. W. Snyder, D. G. Weismiller, and K. V. Holmes.** 1992. Coronavirus species specificity: murine coronavirus binds to a mouse-specific epitope on its carcinoembryonic antigen-related receptor glycoprotein. J. Virol. **66:**7420–7428.
8. **Damico, R. L., J. Crane, and P. Bates.** 1998. Receptor-triggered membrane association of a model retroviral glycoprotein. Proc. Natl. Acad. Sci. USA **95:**2580–2585.
9. **Daniel, C., R. Anderson, M. J. Buchmeier, J. O. Fleming, W. J. Spaan, H. Wege, and P. J. Talbot.** 1993. Identification of an immunodominant linear neutralization domain on the S2 portion of the murine coronavirus spike glycoprotein and evidence that it forms part of complex tridimensional structure. J. Virol. **67:**1185–1194.
10. **Das Sarma, J., L. Fu, J. C. Tsai, S. R. Weiss, and E. Lavi.** 2000. Demyelination determinants map to the spike glycoprotein gene of coronavirus mouse hepatitis virus. J. Virol. **74:**9206–9213.
11. **de Groot, R. J., W. Luytjes, M. C. Horzinek, B. A. van der Zeijst, W. J. Spaan, and J. A. Lenstra.** 1987. Evidence for a coiled-coil structure in the spike proteins of coronaviruses. J. Mol. Biol. **196:**963–966.
12. **Delmas, B., J. Gelfi, R. L'Haridon, L. K. Vogel, H. Sjostrom, O. Noren, and H. Laude.** 1992. Aminopeptidase N is a major receptor for the enteropathogenic coronavirus TGEV. Nature **357:**417–420.
13. **Doms, R. W., R. A. Lamb, J. K. Rose, and A. Helenius.** 1993. Folding and assembly of viral membrane proteins. Virology **193:**545–562.
14. **Dveksler, G. S., C. W. Dieffenbach, C. B. Cardellichio, K. McCuaig, M. N. Pensiero, G. S. Jiang, N. Beauchemin, and K. V. Holmes.** 1993. Several members of the mouse carcinoembryonic antigen-related glycoprotein family are functional receptors for the coronavirus mouse hepatitis virus-A59. J. Virol **67:**1–8.
15. **Dveksler, G. S., M. N. Pensiero, C. B. Cardellichio, R. K. Williams, G. S. Jiang, K. V. Holmes, and C. W. Dieffenbach.** 1991. Cloning of the mouse hepatitis virus (MHV) receptor: expression in human and hamster cell lines confers susceptibility to MHV. J. Virol. **65:**6881–6891.
16. **Dveksler, G. S., M. N. Pensiero, C. W. Dieffenbach, C. B. Cardellichio, A. A. Basile, P. E. Elia, and K. V. Holmes.** 1993. Mouse hepatitis virus strain A59 and blocking antireceptor monoclonal antibody bind to the N-terminal domain of cellular receptor. Proc. Natl. Acad. Sci. USA **90:**1716–1720.
17. **Fischer, F., C. F. Stegen, C. A. Koetzner, and P. S. Masters.** 1997. Analysis of a recombinant mouse hepatitis virus expressing a foreign gene reveals a novel aspect of coronavirus transcription. J. Virol. **71:**5148–5160.
18. **Gallagher, T. M.** 1997. A role for naturally occurring variation of the murine coronavirus spike protein in stabilizing association with the cellular receptor. J. Virol. **71:**3129–3137.
19. **Gallagher, T. M., and M. J. Buchmeier.** 2001. Coronavirus spike proteins in viral entry and pathogenesis. Virology **279:**371–374.
20. **Gallagher, T. M., M. J. Buchmeier, and S. Perlman.** 1992. Cell receptor-independent infection by a neurotropic murine coronavirus. Virology **191:** 517–522.
21. **Godfraind, C., S. G. Langreth, C. B. Cardellichio, R. Knobler, J. P. Coutelier, M. Dubois-Dalcq, and K. V. Holmes.** 1995. Tissue and cellular distribution of an adhesion molecule in the carcinoembryonic antigen family that serves as a receptor for mouse hepatitis virus. Lab. Investig. **73:**615–627.
22. **Gombold, J. L., S. T. Hingley, and S. R. Weiss.** 1993. Fusion-defective mutants of mouse heaptitis virus A59 contain a mutation in the spike protein cleavage signal. J. Virol. **67:**4504–4512.
23. **Hernandez, L. D., R. J. Peters, S. E. Delos, J. A. Young, D. A. Agard, and J. M. White.** 1997. Activation of a retroviral membrane fusion protein: soluble receptor-induced liposome binding of the ALSV envelope glycoprotein. J. Cell Biol. **139:**1455–1464.
24. **Hingley, S. T., J. L. Gombold, E. Lavi, and S. R. Weiss.** 1994. MHV-A59 fusion mutants are attenuated and display altered hepatotropism. Virology **200:**1–10.
25. **Koetzner, C. A., M. M. Parker, C. S. Ricard, L. S. Sturman, and P. S. Masters.** 1992. Repair and mutagenesis of the genome of a deletion mutant of the murine coronavirus mouse hepatitis virus by targeted RNA recombination. J. Virol. **66:**1841–1848.

26. **Krueger, D. K., S. M. Kelly, D. N. Lewicki, R. Ruffolo, and T. M. Gallagher.** 2001. Variations in disparate regions of the murine coronavirus spike protein impact the initiation of membrane fusion. J. Virol. **75:**2792–2802.
27. **Kubo, H., Y. K. Yamada, and F. Taguchi.** 1994. Localization of neutralizing epitopes and the receptor binding site within the amino-terminal 330 amino acids of the murine coronavirus spike protein. J. Virol. **68:**5404–5410.
28. **Kuo, L., G. J. Godeke, M. J. Raamsman, P. S. Masters, and P. J. Rottier.** 2000. Retargeting of coronavirus by substitution of the spike glycoprotein ectodomain: crossing the host cell species barrier. J. Virol. **74:**1393–1406.
29. **Lavi, E., D. H. Gilden, Z. Wroblewska, L. B. Rorke, and S. R. Weiss.** 1984. Experimental demyelination produced by the A59 strain of mouse hepatitis virus. Neurology **34:**597–603.
30. **Lavi, E., E. M. Murray, S. Makino, S. A. Stohlman, M. M. C. Lai, and S. R. Weiss.** 1990. Determinants of coronavirus MHV pathogenesis are localized to 3′ portions of the genome as determined by ribonucleic acid-ribonucleic acid recombination. Lab. Investig. **62:**570–578.
31. **Leparc-Goffart, I., S. T. Hingley, M.-M. Chua, J. Phillips, E. Lavi, and S. R. Weiss.** 1998. Targeted recombination within the spike gene of murine coronavirus mouse hepatitis virus-A59: Q159 is a determinant of hepatotropism. J. Virol. **72:**9628–9636.
32. **Luo, Z., A. M. Matthews, and S. R. Weiss.** 1999. Amino acid substitutions within the leucine zipper domain of the murine coronavirus spike protein cause defects in oligomerization and the ability to induce cell-to-cell fusion. J Virol **73:**8152–8159.
33. **Luo, Z., and S. R. Weiss.** 1998. Roles in cell-to-cell fusion of two conserved hydrophobic regions in the murine coronavirus spike protein. Virology **244:** 483–494.
34. **Makino, S., J. O. Fleming, J. G. Keck, S. A. Stohlman, and M. M. Lai.** 1987. RNA recombination of coronaviruses: localization of neutralizing epitopes and neuropathogenic determinants on the carboxyl terminus of peplomers. Proc. Natl. Acad. Sci. USA **84:**6567–6571.
35. **Matsuyama, S., and F. Taguchi.** 2000. Impaired entry of soluble receptor-resistant mutants of mouse hepatitis virus into cells expressing MHVR2 receptor. Virology **273:**80–89.
36. **Nedellec, P., G. S. Dveksler, E. Daniels, C. Turbide, B. Chow, A. A. Basile, K. V. Holmes, and N. Beauchemin.** 1994. Bgp2, a new member of the carcinoembryonic antigen-related gene family, encodes an alternative receptor for mouse hepatitis viruses. J. Virol. **68:**4525–4237.
37. **Ohtsuka, N., and F. Taguchi.** 1997. Mouse susceptibility to mouse hepatitis virus infection is linked to viral receptor genotype. J. Virol. **71:**8860–8863.
38. **Parker, S. E., T. M. Gallagher, and M. J. Buchmeier.** 1989. Sequence analysis reveals extensive polymorphism and evidence of deletions within the E2 glycoproteins of several strains of murine hepatitis virus. Virology **173:**664–673.
39. **Phillips, J. J., M. Chua, S. H. Seo, and S. R. Weiss.** 2001. Multiple regions of the murine coronavirus spike glycoprotein influence neurovirulence. J. Neurovirol. **7:**421–431.
40. **Phillips, J. J., M. M. Chua, E. Lavi, and S. R. Weiss.** 1999. Pathogenesis of chimeric MHV4/MHV-A59 recombinant viruses: the murine coronavirus spike protein is a major determinant of neurovirulence. J. Virol. **73:**7752–7760.
41. **Rao, P. V., S. Kumari, and T. M. Gallagher.** 1997. Identification of a contiguous 6-residue determinant in the MHV receptor that controls the level of virion binding to cells. Virology **229:**336–348.
42. **Robitaille, J., L. Izzi, E. Daniels, B. Zelus, K. V. Holmes, and N. Beauchemin.** 1999. Comparison of expression patterns and cell adhesion properties of the mouse biliary glycoproteins Bbgp1 and Bbgp2. Eur. J. Biochem. **264:**534–544.
43. **Saeki, K., N. Ohtsuka, and F. Taguchi.** 1997. Identification of spike protein residues of murine coronavirus responsible for receptor-binding activity by use of soluble receptor-resistant mutants. J. Virol. **71:**9024–9031.
44. **Sanchez, C. M., A. Izeta, J. M. Sanchez-Morgado, S. Alonso, I. Sola, M. Balasch, J. Plana-Duran, and L. Enjuanes.** 1999. Targeted recombination demonstrates that the spike gene of transmissible gastroenteritis coronavirus is a determinant of its enteric tropism and virulence. J. Virol. **73:**7607–7618.
45. **Sawa, H., K. Kamada, H. Sato, S. Sendo, A. Kondo, I. Saito, M. Edlund, and B. Obrink.** 1994. C-CAM expression in the developing rat central nervous system. Brain Res. Dev. Brain Res. **78:**35–43.
46. **Spaan, W. J. M., D. Cavanagh, and M. C. Horzinek.** 1988. Coronaviruses. Structure and genome expression. J. Gen. Virol. **69:**2939–2952.
47. **Stauber, R., M. Pfleiderera, and S. G. Siddell.** 1993. Proteolytic cleavage of the murine coronavirus surface glycoprotein is not required for infectivity. J. Gen. Virol. **74:**183–191.
48. **Taguchi, F., H. Kubo, H. Takahashi, and H. Suzuki.** 1995. Localization of neurovirulence determinant for rats on the S1 subunit of murine coronavirus JHMV. Virology **208:**67–74.
49. **Tresnan, D. B., R. Levis, and K. V. Holmes.** 1996. Feline aminopeptidase N serves as a receptor for feline, canine, porcine, and human coronaviruses in serogroup I. J. Virol. **70:**8669–8674.
50. **Weiner, L. P.** 1973. Pathogenesis of demyelination induced by a mouse hepatitis virus (JHM virus). Arch. Neurol. **28:**298–303.
51. **Weismiller, D. G., L. S. Sturman, M. J. Buchmeier, J. O. Fleming, and K. V. Holmes.** 1990. Monoclonal antibodies to the peplomer glycoprotein of coronavirus mouse hepatitis virus identify two subunits and detect a conformational change in the subunit released under mild alkaline conditions. J. Virol. **64:**3051–3055.
52. **Wessner, D. R., P. C. Shick, J. H. Lu, C. B. Cardellichio, S. E. Gagneten, N. Beauchemin, K. V. Holmes, and G. S. Dveksler.** 1998. Mutational analysis of the virus and monoclonal antibody binding sites in MHVR, the cellular receptor of the murine coronavirus mouse hepatitis virus strain A59. J. Virol. **72:**1941–1948.
53. **Yeager, C. L., R. A. Ashmun, R. K. Williams, C. B. Cardellichio, L. H. Shapiro, A. T. Look, and K. V. Holmes.** 1992. Human aminopeptidase N is a receptor for human coronavirus 229E. Nature **357:**420–422.
54. **Yokomori, K., and M. M. C. Lai.** 1992. The receptor for mouse hepatitis virus in the resistant mouse strain SJL is functional: implications for the requirement of a second factor for viral infection. J. Virol. **66:**6931–6938.
55. **Zelus, B. D., J. H. Schickli, D. M. Blau, S. R. Weiss, and K. V. Holmes.** 2003. Conformational changes in the spike glycoprotein of murine coronavirus are induced at 37°C either by soluble murine CEACAM1 receptors or by pH 8. J. Virol. **77:**830–840.
56. **Zelus, B. D., D. R. Wessner, R. K. Williams, M. N. Pensiero, F. T. Phibbs, M. deSouza, G. S. Dveksler, and K. V. Holmes.** 1998. Purified, soluble recombinant mouse hepatitis virus receptor, Bgp1(b), and Bgp2 murine coronavirus receptors differ in mouse hepatitis virus binding and neutralizing activities. J. Virol. **72:**7237–7244.